

Luminescent properties and thermal stability of $\text{BaMgAl}_{10}\text{O}_{17}:\text{Eu}^{2+}$ synthesized by sol–gel route

Peifen Zhu^{a,b}, Weihua Di^{a,*}, Qiren Zhu^b, Baojiu Chen^c, Hongyang Zhu^b,
Haifeng Zhao^a, Yujun Yang^b, Xiaojung Wang^a

^a Key Lab of Excited-State Processes, Changchun Institute of Optics, Fine Mechanics and Physics,
Chinese Academy of Sciences, Changchun 130033, PR China

^b Institute of Atomic and Molecular Physics, Jilin University, Changchun 130012, PR China

^c Department of Physics, Dalian Maritime University, Dalian 116026, PR China

Received 11 May 2006; received in revised form 22 November 2006; accepted 5 December 2006

Available online 22 January 2007

Abstract

$\text{BaMgAl}_{10}\text{O}_{17}:\text{Eu}^{2+}$ (BAM) phosphor particles were prepared by sol–gel processes. The effect of the firing temperature and the Eu^{2+} concentration on the distribution of Eu^{2+} among different sites was firstly investigated through the changes of excitation spectra with changing firing temperature and Eu^{2+} concentration. The mechanism underlying was elucidated. The stability of BAM could be improved by increasing the firing temperature and Eu^{2+} concentration.

© 2006 Elsevier B.V. All rights reserved.

Keywords: BAM; Sol–gel processes; Sites; Stability; Luminescence

1. Introduction

Phosphors are widely used in plasma display panels (PDPs), field emission displays (FEDs), and fluorescence lamps (FLs), etc. [1,2]. $\text{BaMgAl}_{10}\text{O}_{17}$ is an excellent matrix for phosphors because of its chemical stability. For example, the $\text{BaMgAl}_{10}\text{O}_{17}:\text{Eu}^{2+}$ (BAM) as an efficient blue emission phosphor has been used in FLs because it has a deep blue color and a short decay time [3]. It is well known that in FL manufacturing, BAM, which spreads on the insides of a glass tub, is heated at 700–750 °C in air. The PDP manufacturing process also heats phosphor at 500–600 °C to make phosphor layers. These heat-treatments result in the luminance decrease [4]. This is a critical problem in manufacturing of FLs and PDPs. Unlike the other red and green phosphors, only the BAM phosphor shows a considerable decrease in luminescence after heating process [5]. So, the deterioration of its luminescence upon heating is one of the most significant shortcomings in application. The stability of BAM should be improved in order to improve the performance of FL and PDP.

The structure of $\text{BaMgAl}_{10}\text{O}_{17}$, or β -alumina, consists of two spinel blocks (MgAl_2O_4) separated by one mirror plane (BaO) [6]. When Eu^{2+} is substituted into the host lattice, it can have been three possible locations: Beevers–Ross (BR), anti-Beevers–Ross (a-BR), and mid-oxygen (mO) sites in the mirror plane [7]. Peak fitting results show that the primary emission center is assigned to Eu^{2+} on the normal Ba site (the BR site in the cation layer), while the second center is assigned to Eu^{2+} on the a-BR site. The third center has been assigned alternatively to Eu^{2+} in the spinel block, to Eu^{2+} on the mid-oxygen sites in the cation layer, or to Eu^{2+} associated with defect center in the lattice, But it is not populated in the fresh samples [7]. On the mechanism of the deterioration, much research has been conducted. In the literature, luminance deterioration is usually attributed to the oxidation of $\text{BaMgAl}_{10}\text{O}_{17}:\text{Eu}^{2+}$ phosphor and the changes of the environments surrounding the europium ion [3–5]. They indicated that by oxidation, $\text{BaMgAl}_{10}\text{O}_{17}:\text{Eu}^{2+}$ was converted into a mixture of two compounds $\text{BaMgAl}_{10}\text{O}_{17}$ and $\text{Eu}(\text{III})\text{MgAl}_{11}\text{O}_{19}$. This deactivated the Eu^{2+} luminescent center and decreased the Eu^{2+} emission. The important thing that should be noted is that the Eu^{3+} no longer prefers to substitute for the Ba^{2+} , as the Eu^{2+} does. Instead it would prefer to substitute for an aluminum ion in the Al (2) positions, that is, a tetrahedral

* Corresponding author. Tel.: +86 431 6176338; fax: +86 431 6176338.
E-mail address: weihdi@yahoo.com.cn (W. Di).

site. The computer simulation results show that Eu^{2+} prefers to occupy the BR site in the cation layer while Eu^{3+} prefers the Al (2) tetrahedral position in the spinel block [18]. Recently, some other opinions were demonstrated, such as generation of a lattice vacancy [8], migration of Eu^{2+} to the spinel block [9], intercalating water molecules into the host lattice [10], and the transfer of the electron from the divalent europium ions to adsorbed oxygen ions [11]. To the best of our knowledge, there was no report on the influence of the annealing temperature and the Eu^{2+} concentration on the distribution of Eu^{2+} among different sites and its luminescence properties.

In this work $\text{BaMgAl}_{10}\text{O}_{17}:\text{Eu}^{2+}$ is synthesized by sol-gel route. The influence of the annealing temperature and the Eu^{2+} concentration on the distribution of Eu^{2+} among different sites was investigated. The stability of BAM is improved by increasing firing temperature and Eu^{2+} concentration.

2. Experimental

Eu_2O_3 (A-R), $\text{Al}(\text{NO}_3)_3 \cdot 9\text{H}_2\text{O}$ (A-R), $\text{Ba}(\text{NO}_3)_2$ (G-R), $\text{Mg}(\text{NO}_3)_2 \cdot 6\text{H}_2\text{O}$ (A-R), and $\text{C}_6\text{H}_8\text{O}_7 \cdot \text{H}_2\text{O}$ (A-R) were used as starting materials. Europium nitrate solution was obtained by dissolving analytical grade Eu_2O_3 in dilute nitric acid. Then a stoichiometric amount of metal nitrates were dissolved in distilled water. Subsequently, a weighed quantity of citric acid ($\text{C}_6\text{H}_8\text{O}_7 \cdot \text{H}_2\text{O}$) was added to the nitrate solution. The mole ratio of citric acid to the total concentration of metal ions was adjusted to 1.5. After mixing, homogenous colorless solution was obtained. 3 h later, the 30% ammonia was added to the solution and the pH was adjusted to 5–6. The water was slowly evaporated off from solution at 110°C and a dark metal citrate suspension was formed at first. Further heating 1 h result in dark colored amorphous citrate gels with high viscosity, which were then calcined at 700°C for 2 h in air to remove organic residues. The calcined powder was, respectively, heated at 1250, 1350 and 1450°C for 2 h under a reducing atmosphere (CO). In another experiment, the calcined powder was annealed at 1350°C in air, and then heated in reducing atmosphere, respectively, at 600, 700, 750, 800, 900, 1000, 1100, and 1300°C .

In the same way, $\text{Ba}_{1-x}\text{Eu}_x\text{MgAl}_{10}\text{O}_{17}$ ($x=0.01, 0.05, 0.1$, and 0.18) precursors were obtained. These precursors were calcined at 700°C for 2 h in air, and then heated at 1350°C for 2 h under a reducing atmosphere.

Finally, all the as-prepared samples are annealed at different temperatures for some time in air.

XRD studies were conducted on a Rigaku D/max-2000 X-ray powder diffractometer with $\text{Cu K}\alpha$ radiation. The emission and excitation spectra at room temperature were measured with a Hitachi F-4500 fluorescence spectrometer.

3. Results and discussion

3.1. XRD and photoluminescence analysis

In order to understand the relationship between the luminescence characteristics and the crystallization behavior of BAM from amorphous citrate precursor, temperature-resolved X-ray diffraction patterns and photoluminescence (PL) spectra were measured, as represented in Fig. 1. The precursor fired at 1150°C in reducing atmosphere only shows characteristic of a certain unknown phase (see Fig. 1(a)), correspondingly, its emission spectrum is shown in Fig. 2(b). The peaks observed are characteristics of the $^5\text{D}_0 \rightarrow ^7\text{F}_{J(J=0-4)}$ transition of Eu^{3+} , no blue emission is observed yet. This indicates that this unknown phase obtained at 1150°C is a certain Eu^{3+} -containing compound. When the temperature increases to 1250°C , the characteristics of diffraction peaks of BAM appear without any other impurities

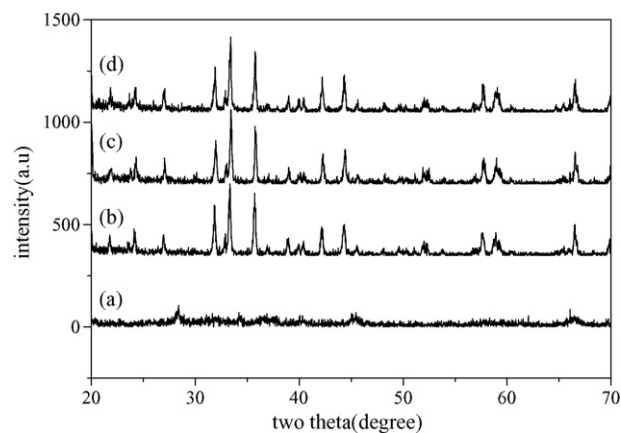


Fig. 1. XRD patterns of the $\text{Ba}_{0.9}\text{Eu}_{0.1}\text{MgAl}_{10}\text{O}_{17}$ sintered at different temperatures in reducing atmosphere. (a) 1150°C , (b) 1250°C , (c) 1350°C , and (d) 1450°C .

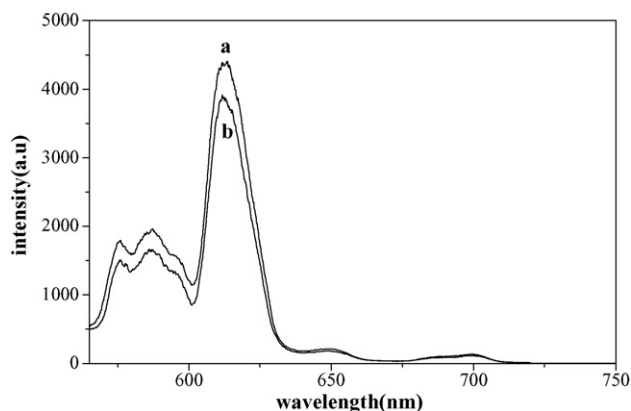


Fig. 2. Emission spectra of the precursors sintered at (a) 1050°C , and (b) 1150°C in reducing atmospheres under 254 nm excitation.

(see Fig. 1(b)) and the red emission is no longer observed, but we observed the blue emission peaking at 450 nm as illustrated in the Fig. 3(c). Fig. 3 is the emission spectrum under 254 nm excitation, which consists of a wide band peaking at 450 nm (the blue emission), corresponding to $5\text{d} \rightarrow 4\text{f}$ transitions of the Eu^{2+} . The

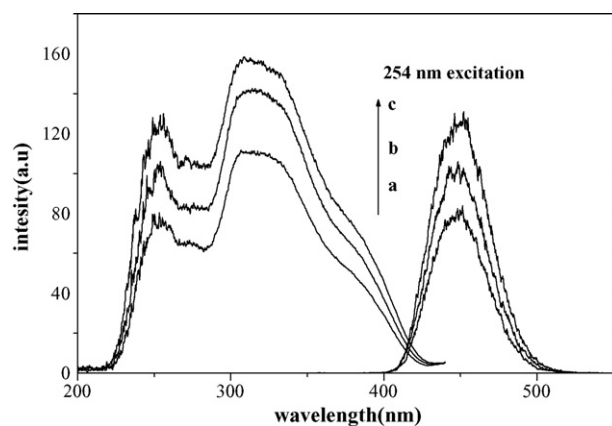


Fig. 3. Emission spectra under 254 nm excitation and excitation spectra monitoring the 450 nm emission of $\text{Ba}_{0.9}\text{Eu}_{0.1}\text{MgAl}_{10}\text{O}_{17}$ synthesized at (a) 1250°C , (b) 1350°C and (c) 1450°C .

excitation spectrum monitoring 450 nm emission is also shown in Fig. 3, the two wide bands peaking at about 250 and 310 nm, respectively, is due to the field splitting of the Eu^{2+} d-orbital [12]. This indicates that the unknown Eu^{3+} -related phase has been transited to BAM phase going from 1150 to 1250 °C in reducing atmosphere and Eu^{3+} has also been reduced to Eu^{2+} in this process. The preparation of BAM using solid-state reaction commonly requires a temperature as high as at least 1500 °C, but it can be synthesized at 1250 °C using sol–gel processes. This indicates that the use of sol–gel can decrease the firing temperature, also, it can effectively control the size and morphology of BAM particles [13]. Further increasing the firing temperature to 1350 and 1450 °C, no appreciable changes in the diffraction patterns are observed except for a little increased intensity (see Fig. 1(c) and (d)), correspondingly, in the emission spectrum, only the intensity increased and no other changes take place, as shown in Fig. 3. All the results indicated that the luminescence intensity of BAM phosphor was affected by firing temperature in a reducing atmosphere.

The effects of heating atmosphere on the luminescent properties of the phosphor are also investigated. Fig. 4 illustrates the excitation (monitor 450 nm emission) and emission (under 310 nm excitation) spectra for the sol–gel derived $\text{Ba}_{0.82}\text{Eu}_{0.18}\text{MgAl}_{10}\text{O}_{17}$ phosphors which are first calcined at 1350 °C in the air and then annealed at different temperatures in reducing atmosphere. The PL spectra shown from 590 to 700 nm in the inset of Fig. 4, corresponding to the nature of transition of Eu^{3+} , decreased with increasing annealing temperature. The emission from Eu^{2+} is not obviously observed since a very small amount of Eu^{3+} is reduced to Eu^{2+} at lower annealing temperatures. However, the blue emissions peaking at 450 nm appear at 900 °C, and increasing significantly with increasing temperature. In addition to PL, the reducing process is also detected from electron paramagnetic resonance spectroscopy (EPR) and Eu L_{III}-edge X-ray absorption near edge structure (XANES) [13,14]. But our interest is mainly focused on the relative intensity of these two excitation bands of Eu^{2+} . As previously indicated, there are two wide bands one located at

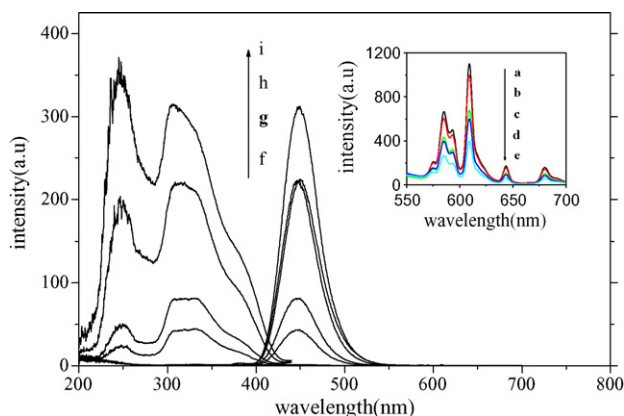


Fig. 4. The excitation spectra of $\text{Ba}_{0.82}\text{Eu}_{0.18}\text{MgAl}_{10}\text{O}_{17}$ monitoring the blue emission peaking at 450 nm (left) and the emission spectra under 310 nm excitation (right) first fired at 1350 °C in air and then annealed in reducing atmosphere at different temperatures: (a) no annealing process, (b) 600 °C, (c) 700 °C, (d) 750 °C, (e) 800 °C, (f) 900 °C, (g) 1000 °C, (h) 1100 °C and (i) 1300 °C.

short wavelength peaking at 250 nm and the other at long wavelength peaking at 310 nm. As annealing temperature increases, the overall intensity increases, as expected. In addition, long wavelength excitation generates more emission than short wavelength excitation at lower annealing temperatures. At 1100 °C, the relative excitation intensities in the two regions are about the same, and further increasing the annealing temperature to 1300 °C, the short wavelength excitation becomes more efficient. In order to understand the underlying mechanisms, one needs to know the location and environment of activator ions in the host lattices. Multiple sites for europium have been proposed and proved employing different methods [15–17]. Wu and Cormack [18] employing computer simulation found that energetically, Eu^{2+} prefers to occupy the BR site in the cation layer while Eu^{3+} prefers to occupy the Al (2) site in the middle of the spinel block. Since the Eu^{3+} ions occupy Al (2) sites in the middle of the spinel block and the Eu^{2+} ions occupy the BR site in the mirror plane, it is necessary for europium to migrate from the Al (2) site to the BR site in the process of the reduction from Eu^{3+} to Eu^{2+} . However, there is about 5 Å distances between both sites [18], to migrate, europium must obtain certain energy. In Fig. 5, when the annealing temperature is lower than 900 °C, due to the Eu^{3+} occupying the Al (2) site in the middle of the spinel block, it could not obtain enough energy to migrate to the mirror plane at relatively low temperature and the Eu^{3+} is not reduced to Eu^{2+} , therefore we could not observe the blue emission. More and more Eu^{3+} obtaining enough energy migrate to the cation layer with increasing the temperature and at the same time the Eu^{3+} is reduced to Eu^{2+} , therefore, the blue emission is observed and becomes stronger with increasing temperatures. In order to clarify the assignment of emission centers in BAM, Pike et al. [7,19] fit the Eu^{2+} emission spectra. The primary emission center is assigned to the Eu^{2+} on the normal Ba site (the BR site in the cation layer), while the second center is assigned to Eu^{2+} on the a-BR site. The third center does not exist in the fresh samples. In Fig. 4, the changes of excitation spectra with increasing the annealing temperature are likely related to sites occupied by Eu^{2+} . Since the a-BR site is small in comparison to BR site [18]. The smaller is the size of interstitial position, the bigger the energy needed to accommodate the interstitial ion. So, the Eu^{2+}

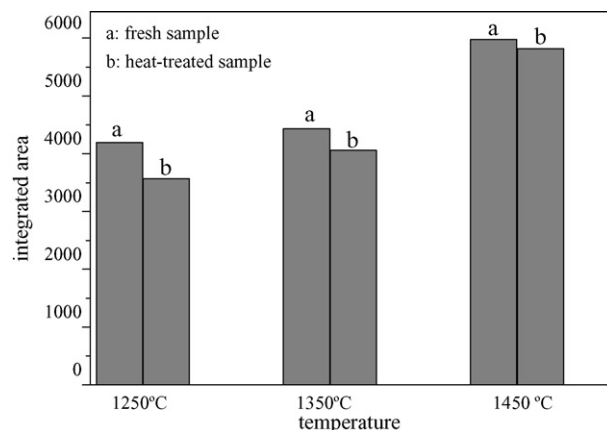


Fig. 5. The integrated emission intensity of fresh and heat-treated samples as a function of firing temperature.

ions occupy the BR sites first at relatively low annealing temperatures. Therefore, the BR site is the most energetically favorable site for Eu^{2+} . More and more Eu^{3+} are released from the A (2) site to the Ba site and reduced to Eu^{2+} with increasing annealing temperature in a reducing atmosphere and at the same time more and more Eu^{2+} migrating from Al (2) sites or BR sites would occupy the a-BR sites other than BR sites. The distribution of Eu^{2+} is not random [19]. So, when the annealing temperature is low, the Eu^{2+} mainly occupy the BR site and the Eu^{2+} tend to occupy both BR sites and a-BR sites with increased temperature. The two wide bands originate from the transitions from the $4f^7$ ground state of the Eu^{2+} to the T_{2g} and E_g excited states of the $4f^65d$ configuration [20,21]. Relative rate of transition to T_{2g} and E_g should be different because the environment surrounding the Eu^{2+} is different. The excitation spectra (see Fig. 3) demonstrate that the BR site excitation is more effective in the long wavelength peaking at 310 nm, but the a-BR site is more effective in the short wavelength peaking at 250 nm. As previously indicated, the ratio of a-BR site to BR site is increased with increasing the annealing temperature. Therefore, the long wavelength excitation at 310 nm is more effective at lower annealing temperature, but the short wavelength excitation is more effective at higher temperature (see Fig. 4). The experimental results are well consistent with our proposal. Based on our results, we proposed a model of the reducing process: (1) the Eu^{3+} located in the Al (2) sites absorb some energy, (2) it migrate from the Al (2) site to the BR site, (3) $\text{Eu}^{3+} \rightarrow \text{Eu}^{2+}$, (4) the Eu^{2+} at the BR site absorb more energy, (5) the migration of Eu^{2+} from the BR site to the a-BR site. Finally the Eu^{2+} ions occupy more than one sites.

3.2. The influence of crystallinity on the stability of $\text{BaMgAl}_{10}\text{O}_{17}:\text{Eu}^{2+}$

Fig. 5 shows the effects of thermal damage on the emission spectra of sol-gel derived $\text{Ba}_{0.9}\text{Eu}_{0.1}\text{MgAl}_{10}\text{O}_{17}$, which crystallized at different temperatures, respectively, at 1250, 1350, and 1450 °C in reducing atmosphere. From above figure it was found that after annealing at 600 °C, the emission intensity decreased at the same time in these three samples, but the decreasing rate is different. The sample crystallized at 1250 °C decreases to about 85.1% of the integrated brightness of the fresh sample after annealing at 600 °C, while the samples crystallized at 1350 and 1450 °C decrease to 91.7 and 97.4%, respectively, after annealing at 600 °C. All these indicate that the well-crystallized samples can be obtained at high temperature and better-crystallized samples are helpful to maintenance of emission under thermal treatment. To understand the mechanism between the maintenance and firing temperature, we also should know the location and environment of activators in the host matrix. As we previously analyzed, Eu^{2+} has more than one site in BAM. When the temperature is low, most of the Eu^{2+} ions occupy the BR sites because it is easier for Eu^{3+} migrate to the BR than to a-BR site. But when the firing temperature is higher, the Eu^{2+} will migrate from the BR site to anti-BR site. Therefore, ratio of a-BR site to BR site increased with increasing the temperature. Because the luminance decrease is due to oxi-

dation of $\text{BaMgAl}_{10}\text{O}_{17}:\text{Eu}^{2+}$, and a-BR site is smaller than BR site, it is more difficult for O_2 to occupy the a-BR site than BR site. Therefore, the a-BR site is more stable. This is consistent with conclusion of Stephan et al. [22]. It is not difficult to understand the tendency illustrated in Fig. 5. Zhang et al. [23] also indicated that the highly crystallized $\text{BaMgAl}_{10}\text{O}_{17}:\text{Eu}^{2+}$ are resistance to the deterioration of the luminescence during baking process. This is consistent with phosphors under VUV damage [23,24]. They proved that improvement in the crystallization of BAM phosphor would not only enhance its emission efficiency but also decrease the deterioration during VUV irradiation. These Eu^{2+} ions are relatively more stable in more crystalline samples.

In conclusion, highly crystallized BAM can be obtained when annealing the precursor at 1450 °C in reducing atmosphere and the BAM with higher crystallinity is relatively more stable to thermal damage. Deterioration process of BAM could be decreased if the phosphor is synthesized with high crystallinity. The high crystallinity is helpful for Eu^{2+} to occupy relatively stable sites.

3.3. The influence of concentration of Eu on the thermal degradation

To understand the effect of europium content on luminescence properties of sol-gel derived phosphors, photoluminescence studies are carried out for $\text{BaMgAl}_{10}\text{O}_{17}$ doped with different concentrations of Eu^{2+} . Fig. 6 illustrates the excitation ($\lambda = 450$ nm) and emission ($\lambda = 254$ nm) spectra recorded for $\text{Ba}_{1-x}\text{Eu}_x\text{MgAl}_{10}\text{O}_{17}$ containing different amount of x where $x = 0.01, 0.05, 0.1$, and 0.18 . UV-induced luminescence increases with elevated concentration of Eu^{2+} .

The excitation spectrum consists of two broad bands centered at 250 and 310 nm, respectively. As the Eu^{2+} concentration increases, the overall intensity increases, as expected. However, the ratio of the intensity of these two bands varies significantly. At a lower concentration of Eu^{2+} , the intensity of the band peaking at 310 nm is much higher than that of the band peaking at

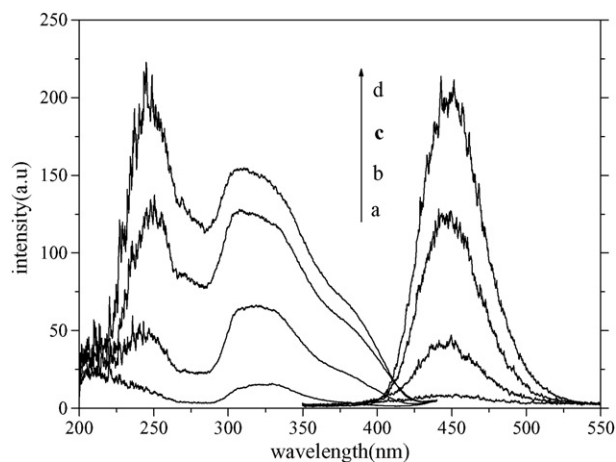


Fig. 6. The excitation spectra monitoring the blue emission peaking at 450 nm and the emission spectra under 254 nm excitation of $\text{Ba}_{1-x}\text{Eu}_x\text{MgAl}_{10}\text{O}_{17}$ ($x = 0.01, 0.05, 0.1$ and 0.18): (a) $x = 0.01$, (b) $x = 0.05$, (c) $x = 0.1$, and (d) $x = 0.18$.

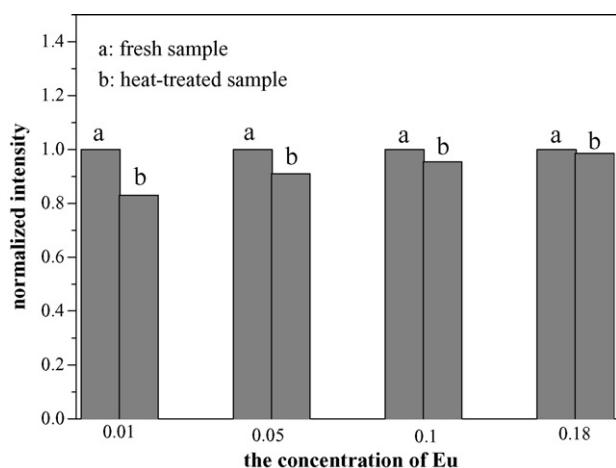


Fig. 7. The integrated emission intensity of the fresh and heat-treated sample as a function of the concentration of Eu^{2+} .

250 nm. In this case, the excitation at 310 nm is more efficient than that at 250 nm. As the Eu^{2+} concentration increases to 10%, almost equal intensity of these two bands is observed. Further increasing Eu^{2+} concentration to 18%, the intensity of the band at 250 nm is much higher than that of the band at 310 nm, in this case, the excitation at 250 nm is more efficient than that at 310 nm. This may be related to the different sites occupied by Eu^{2+} . As indicated previously, various methods have proved that the Eu^{2+} occupy more than one site. When the Eu is doped into the BAM, The Eu should be preferable to occupy BR site and then occupied the a-BR site. The Eu^{2+} will mainly occupy BR site when the concentration is low, so we only observed the bands centered at 310 nm in 0.01 mole-doped BAM. When the concentration increased to 0.05 mole, the 254 nm excitation is observed. The short wavelength and the long wavelength excitation increased at the same time with increasing concentration, but the short wavelength excitation peaking at 254 nm increased more quickly. At previous part, we have indicated that the a-BR site is more effective in the short wavelength peaking at 250 nm. This indicates that the ratio of Eu^{2+} at a-BR to BR site increased with the concentration of Eu^{2+} .

Fig. 7 shows the effects of thermal damage on emission spectrum of $\text{Ba}_{1-x}\text{MgAl}_{10}\text{O}_{17}:\text{Eu}_x$ ($x=1, 5, 10$ and 18%), respectively. After the thermal damage at 600°C , the samples doped with 1, 5, 10 and 18% Eu decrease to about 83, 91, 95.5 and 98.5%, respectively. As previously indicated, the ratio of Eu^{2+} at a-BR increased with the concentration of Eu^{2+} , energetically the a-BR site appears to be more stable than the other two sites [22]. Therefore, the sample with higher Eu concentration is relatively more stable to thermal damage. Our observation is consistent with what has been reported by Zachau et al. [24] who demonstrated that BAM with 20% Eu^{2+} is more stable than standard BAM which contains about 10% Eu^{2+} . T. Justel [5] also achieved the same conclusion. The sample with higher Eu^{2+} concentration is relatively more stable under baking process. This tendency is consistent with samples damaged by VUV [8]. They found that After the VUV damage, the sample doped at 10% Eu decreases to about 16% of the integrated brightness of the fresh sample, while the sample doped at 1% Eu decrease to

about 8% of fresh. They concluded that: the sample with higher Eu^{2+} loading is relatively more stable to VUV damage. All the results indicated the luminance maintenance could be improved by increasing Eu^{2+} concentration.

4. Conclusion

The $\text{BaMgAl}_{10}\text{O}_{17}:\text{Eu}^{2+}$ was synthesized employing the sol-gel processes. The photoluminescence and stability properties with increasing the firing temperature and Eu^{2+} concentration were investigated. The results indicated that the photoluminescence and the stability increased with increasing the firing temperature and Eu^{2+} concentration. We elucidated the underlying mechanism, which might be related to the multiple sites occupied by Eu^{2+} and these sites have different stability.

Acknowledgements

This work was supported by the National Natural Science Foundation of China (Grant Nos. 50502031, 50572102) and The Young People Foundation of Jilin Province (Grant No. 20060522).

References

- [1] C.R. Ronda, J. Alloy. Compd. 225 (1995) 534.
- [2] W.H. Di, X.J. Wang, B.J. Chen, S.Z. Lu, X.X. Zhao, J. Phys. Chem. B 109 (2005) 13154.
- [3] K.S. Sohn, S.S. Kim, H.D. Park, Appl. Phys. Lett. 81 (2002) 1759.
- [4] S. Oshio, T. Matsuoka, S. Tanaka, H. Kobayashi, J. Electrochem. Soc. 145 (1998) 3903.
- [5] T. Justel, H. Nikol, Adv. Mater. 12 (2000) 527.
- [6] K.B. Kim, Y.I. Kim, H.G. Chun, T.Y. Cho, J.S. Jung, J.G. Kang, Chem. Mater. 14 (2002) 5045.
- [7] B. Dawson, M. Ferguson, G. Marking, A.L. Diaz, Chem. Mater. 16 (2004) 5311.
- [8] H. Yamada, W.S. Shi, C.N. Xu, J. Electrochem. Soc. 151 (2004) E349.
- [9] Y.H. Wang, Z.H. Zhang, Electrochem. Solid State Lett. 8 (2005) H97.
- [10] K.C. Mishra, M. Raukas, G. Marking, P. Chen, P. Boolchand, J. Electrochem. Soc. 152 (2005) H183.
- [11] G. Bizarri, B. Moine, J. Lumin. 113 (2005) 199.
- [12] J.Y. Zhang, Z.T. Zhang, Z.L. Tang, Y. Tao, X. Long, X. Long, Chem. Mater. 14 (2002) 3005.
- [13] Y.I. Kim, S.C. Moon, S.O. Kang, M.J. Jun, J.S. Kang, J. Mater. Sci. Lett. 22 (2003) 669.
- [14] D.K. Kim, S.H. Hwang, I.G. Kim, J.C. Park, S.H. Byeon, J. Solid State Chem. 178 (2005) 1414.
- [15] P. Boolchand, K.C. Mishra, M. Raukas, A. Ellens, P.C. Schmidt, Phys. Rev. B 66 (2002) 134429.
- [16] K.C. Mishra, M. Raukas, A. Ellens, K.H. Johnson, J. Lumin. 96 (2002) 95.
- [17] A. Ellens, F. Zwasschka, F. Kummer, A. Meijerink, M. Raukas, K. Mishra, J. Lumin. 93 (2001) 147.
- [18] Z.H. Wu, A.N. Cormack, J. Electroceram. 10 (2003) 179.
- [19] V. Pike, S. Patraw, A.L. Diaz, B.G. DeBoer, J. Solid State Chem. 173 (2003) 359.
- [20] P. Dorenbos, J. Alloy Compd. 341 (2002) 156.
- [21] T. Ishii, M.G. Brik, K. Ogasawara, J. Alloy Compd. 380 (2004) 136.
- [22] M. Stephan, P.C. Schmidt, K.C. Mishra, M. Raukas, A. Ellens, P. Boolchand, Z. Phys. Chem. 215 (2001) 1397.
- [23] S.S. Zhang, Y.Q. Hou, H. Fujii, T. Onishi, M. Kokubu, M. Obata, H. Tanno, T. Kono, H. Uchiike, Jpn. J. Appl. Phys. 42 (2003) 477.
- [24] M. Zachau, D. Schmidt, U. Mueller, C.F. Chenot, Word Patent WO9934389.